Journal of Iberian Geology **42 (2) 2016:** 187-200
http://dx.doi.org/10.5209/rev_JIGE.2016.v42.n2.52865

www.ucm.es/info/estratig/journal.htm
ISSN (print): 1698-6180. ISSN (online): 1886-7995

Journal of Iberian Geology
AN INTERNATIONAL PUBLICATION OF EARTH SCIENCES

Upper-Pleistocene terrace deposits in Mediterranean climate: geomorphological and source-rock control on mineral and geochemical signatures (Betic Cordillera, SE Spain)

R. Jiménez-Espinosa[1]*, J. Jiménez-Millán[1], F.J. García-Tortosa[1]

[1]*Department of Geology and CEACTierra, Associated Unit IACT (CSIC-UGR), Faculty of Experimental Science, University of Jaén, Campus Las Lagunillas s/n, 23071 Jaén, Spain.*

*e-mail addresses: respino@ujaen.es (R.J.-E, * Corresponding author); jmillan@ujaen.es (J.J.-M.); gtortosa@ujaen.es, (F.J.G.-T.)*

Received: 3 June 2016 / Accepted: 22 July 2016 / Available online: 10 August 2016

Abstract

Mineral and chemical composition of alluvial Upper-Pleistocene deposits from the Alto Guadalquivir Basin (SE Spain) were studied as a tool to identify sedimentary and geomorphological processes controlling its formation. Sediments located upstream, in the north-eastern sector of the basin, are rich in dolomite, illite, MgO and K_2O. Downstream, sediments at the sequence base are enriched in calcite, smectite and CaO, whereas the upper sediments have similar features to those from upstream. Elevated rare-earth elements (REE) values can be related to low carbonate content in the sediments and the increase of silicate material produced and concentrated during soil formation processes in the neighbouring source areas. Mineral characterization and geomorphological setting indicate that physical degradation, short transport and fast physical deposition were prominent processes, suggesting element fractionation effects can be almost neglected and element distribution can be interpreted according to the influence of the source areas. Two mineralogical and geochemical signatures related to different sediment source areas were identified. Basal levels were deposited during a predominantly erosive initial stage, and are mainly composed of calcite and smectite materials enriched in REE coming from Neogene marls and limestones. Then the deposition of the upper levels of the alluvial sequences, made of dolomite and illitic materials depleted in REE coming from the surrounding Sierra de Cazorla area took place during a less erosive later stage of the fluvial system. Such modification was responsible of the change in the mineralogical and geochemical composition of the alluvial sediments.

Keywords: fluvial system, calcite/dolomite ratio, clay minerals, REE patterns, Guadalquivir River, source area

Resumen

Se ha estudiado la composición mineral y química de los depósitos aluviales del Pleistoceno Superior del Alto Guadalquivir (SE de España) como una herramienta para identificar los procesos sedimentarios y geomorfológicos que controlan su formación. Los sedimentos de la parte alta del cauce, en el sector noreste de la cuenca, son ricos en dolomita, illita, MgO y K_2O. Descendiendo en el cauce, los sedimentos de la base de la secuencia están enriquecidos en calcita, esmectita y CaO, mientras que los sedimentos de la parte superior de dicha secuencia tienen características similares a los presentes en la parte superior del cauce. La presencia de sedimentos con elevados valores en elementos de las tierras raras (REE) puede relacionarse con el bajo contenido en carbonatos y el incremento de silicatos producido y concentrado durante los procesos de formación de suelos en las áreas fuente vecinas.

Se identificaron dos patrones mineralógicos y geoquímicos relacionados con los diferentes sedimentos de las áreas fuente. Los niveles basales fueron depositados durante una etapa inicial predominantemente erosiva y están formados principalmente por materiales calcíticos y esmectíticos enriquecidos en REE que proceden de las margas y calizas del Neógeno. Posteriormente, el depósito de los materiales de los niveles superiores de las secuencias aluviales, formados por materiales que proceden del área de la Sierra de Cazorla ricos en dolomita e illita y empobrecidos en REE, tuvo lugar durante una etapa posterior menos erosiva del sistema fluvial. Las modificaciones de las condiciones del sistema fluvial fueron responsables del cambio en la composición geoquímica y mineralógica de los sedimentos aluviales.

Palabras clave: sistema fluvial, razón calcita/dolomita, arcillas, tierras raras, río Guadalquivir, área fuente

1. Introduction

Temporal changes in the depositional environment, tectonic setting, geology of the source area are frequently considered as some of the main factors controlling the characteristics of river sediments (Blank and Margolis, 1975; Anderson and Ashley, 1991; Ehrmann *et al.*, 1992; Grobe and Mackensen, 1992; Yoon *et al.*, 2000; Mehl *et al.*, 2012, Prizomwala *et al.*, 2014). Most of the sedimentological studies focus on the correlation of sediment structures to describe sedimentary processes. However, the mineralogical study in Quaternary sediments constitutes a useful tool to find out information about sedimentary changes (Müller and Stein, 2000; Bayhan, 2005). Dinis and Oliveira (2016) suggested in a recent special issue by Caracciolo *et al.* (2016) that coupling geochemical data with sediment mineralogy and texture should allow tracing complex provenance and evaluating the roles played by other factors besides provenance on sediment composition.

Mineral assemblages in river sediments can be used as fingerprints of the processes that occurred in the drainage area. Many of the changes in these fingerprints are conventionally associated with climate variations (Gingele and De Deckker, 2004). Physically eroded mica/illite and chlorite are generally interpreted to occur under cold climate conditions, whereas smectite and kaolinite are formed from chemical weathering mechanisms under warm and humid climate conditions. Mineral assemblages in continental river sediments are also strongly controlled by the composition of the source rock, transport and depositional mechanisms (Whitmore *et al.*, 2004). The source areas and the type of weathering mechanism control the different clay mineral assemblages, and transport-sedimentation mechanisms may lead to a selective enrichment in the different mineral phases (Chamley, 1989).

Sediment chemical composition and rare-earth elements (REE) signatures might distinguish the provenance of sediments and the intensity of soil erosion processes, especially in carbonate-rich sediments considering the great disparity in REE concentration between carbonate minerals (which are dominated by calcite and dolomite) and soil particles (which are dominated by quartz and clay minerals) (e.g. Wen *et al.,* 2014). Moreover, during the evolution of alluvial systems there can be changes in the active areas of sedimentation as well as in the source areas of the sediments. Tectonic activity is considered to be a major control on these processes by increasing slope gradients through uplift and tilting or by changing the local base-level (Stokes and Mather 2000).

The Upper Pleistocene alluvial terrace deposits of the Quaternary alluvial sediments of the Alto Guadalquivir Basin (SE Spain) provide an excellent example of how geomorphological evolution can exert an important control on mineral and geochemical signatures of sediments in a tectonically active area (Baena 1993; García-Tortosa *et al.*, 2008). The location of the study area among three different main geological units of the Iberian Peninsula (Hercynian Iberian Massif, Tertiary Guadalquivir Basin and External Zone of the Alpine Betic Cordillera) allows to carry out a specific case study to reveal the role of the chemical and physical processes that affect Quaternary alluvial sediment composition (source-rock lithology changes, relief, drainage system, climate, tectonic environment, etc.).

This paper describes a case study that demonstrates the application and utility of the use of detrital mineralogy and geochemistry of sediments to unravel the geomorphic history of a specific locality. The main goals of this study are (1) to describe the nature and distribution of the alluvial terrace deposits of the Quaternary alluvial sediments of the Alto Guadalquivir Basin (SE Spain) based on sedimentary facies as well as on mineral and geochemical evidence, (2) to identify and discriminate different sediment sources of the Guadalquivir River alluvial deposits, (3) to estimate the potential factors that control the observed changes in the mineralogy and geochemistry within the different studied sedimentary sequences, and (4) to propose a terrace deposit model in the light of processes that have interacted to form the terrace sediments.

2. Study area

The climate of the study area, in Jaén province (Southern Spain), is of Mediterranean type, with an average annual precipitation of 375 mm per year (Jiménez-Espinosa and Jiménez-Millán, 2003). During the hot dry summer season (June-August), the climate can be considered arid. Most of the precipitation is concentrated in the winter season (December–January). The study area has a xeric moisture regime. The studied area is located in the north-eastern sector of the Guadalquivir Basin (Fig. 1). This is a foreland basin developed between the Iberian Massif (passive margin) to the north and the front of the Betic Cordillera (active margin) to the south (Figs. 1 and 2), being one of the largest Tertiary basins in the Iberian Peninsula. The Guadalquivir River incises this Tertiary basin. This valley is surrounded by several lithological units: (i) to the north, the Hercynian basement of Sierra Morena comprising a wide variety of Palaeozoic rocks such as granitic plutonic rocks and metamorphic rocks (slates, schists and hornfels), (ii) to the south, the Subbetic domain of the External Zone of the Betic Cordillera (Sierra Mágina), which constitutes a far more abrupt southern margin comprising mainly Mesozoic limestones, and (iii) to the east, the Prebetic domain of the External Zone of the Betic Cordillera (Sierra de Cazorla), incised by the upper stream of the Guadalquivir River and composed of Mesozoic carbonates, predominantly dolostones in the study area.

In the study area, most of the Guadalquivir River stream cut into the marine sedimentary infill of the Neogene basin. This basin comprises several lithostratigraphic units ranging from middle Miocene to Pliocene (Roldán, 1995): Langhian-early Serravallian unit (also known as Olistostromic Unit), late Serravallian-early Tortonian unit, late Tortonian unit, Messinian unit, late Messinian-early Pliocene unit, and Pliocene unit. Except for the Olistostromic Unit, which is composed of

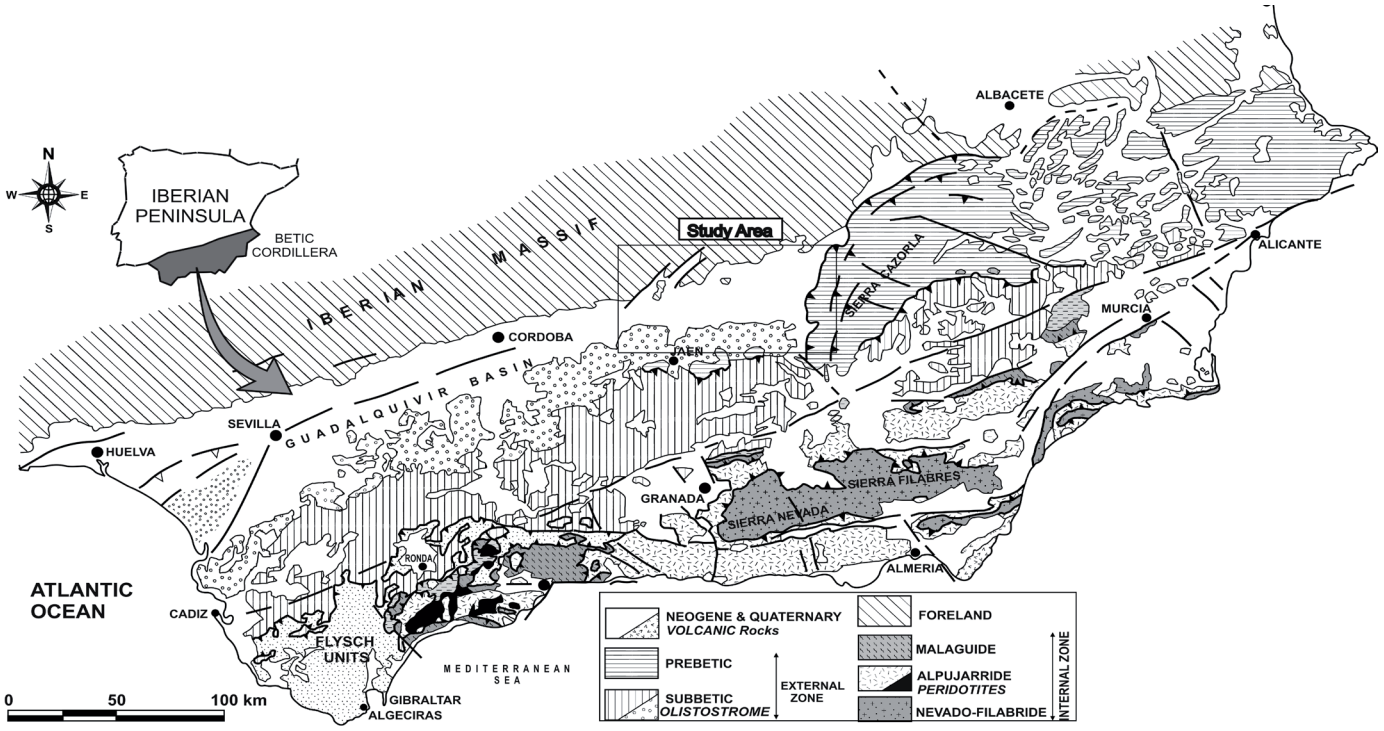

Fig. 1.- Regional geology map showing the location of the study area.

clays, red sandstones, gypsum and dolostones from Triassic units of the front of the External Zone of the Betic Cordillera, the rest of the units comprise deposits of marls, algal limestones, calcarenites and sandstones with carbonate cement, consequently their carbonate content is in general very high. The Olistostromic unit and the late Serravallian-early middle Tortonian unit outcrop in the southern part of the study area. In the northern sector the late Tortonian unit outcrops, from the Sierra de Cazorla to the east of the village of Mengíbar, whereas to the west the Messinian unit outcrops (Fig. 2).

The alluvial Quaternary deposits unconformably overlie the Mio-Pliocene lithological units. They consist of conglomerates, gravels, sands, and silts. The thickness of the alluvial sequence, deposited by the Guadalquivir River and its tributaries, ranges from about 5 to 12 m, although it varies considerably along the basin. In the study area, three levels of fluvial terraces can be differentiated: upper, middle, and lower terrace. Only the uppermost part of the lower terrace can be observed. It consists of silts and fine-grained sands characteristic of the floodplain. The upper terrace is very eroded and their remnants can only be observed at the confluence of the Guadalquivir River with its tributaries Guadalimar, Guadiana Menor and Bedmar, and at about 4 km to the south of the village of Torreblascopedro (Fig. 2). The mineralogical and compositional characterization was carried out on the middle terrace, which is the most extensive of the three terraces. This terrace comprises a fining-upward megasequence with a complex internal structure. In general, the sedimentary facies observed can be grouped in channel facies (basal part) and floodplain facies (upper part). In relation to time constrains, this terrace can be correlated with those dated by Baena (1993) using radiometric, paleontogical, and archaelogical data. Taking into account that this terrace occurs around 25m on the current talweg, an 80 ka age can be suggested. The studied alluvial sediments were sampled at four different mining sites (S1, S2, S4 and S5), which are representative of the whole study area (Fig. 3). These sedimentary sequences overlie three of the aforementioned Neogene lithological units incised by the Guadalquivir River: a block of Triassic dolostones of the Olistostromic unit (S1), marly materials of the Olistostromic unit (S2), the Messinian unit (S4), and the late Tortonian unit (S5) (Figs. 3, 4).

From the geomorphological point of view, in the headwater of the Guadalquivir River, before reaching the Neogene sediments from the Guadalquivir Basin, 60 km of the river early upper segment cross the Sierra de Cazorla thick dolomitic sequence (Figs. 2, 3). In this area, the river turns almost 180º to take the main valley direction in the medium-high segment. Initially, the Guadalquivir valley has a 35 km segment parallel to the NNE-SSW Sierra de Cazorla tectonic orientation structures, turning 90º at the Tranco damming to cross perpendicularly over those tectonic structures for 15 km. 10 km before leaving the Sierra de Cazorla sequence, the river stream becomes progressively parallel to the main valley direction in the Neogene Guadalquivir basin sediments. The geomorphological analysis of the fluvial terraces in the study area showed that the Guadalquivir river middle terrace is very well exposed in the river middle-upper segment, where upper terraces are very scarcely preserved. This middle terrace is ca. 50 m below the relics of higher terraces and more than 200 m down the upper erosive surface described (pediments).

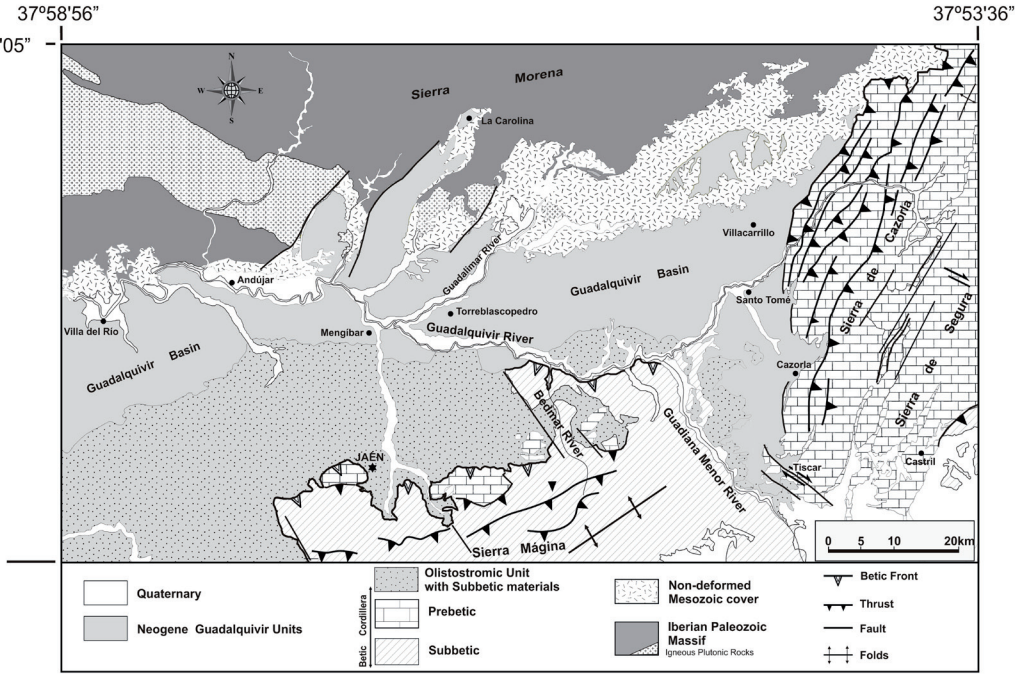

Fig. 2.- Local geology map showing the main lithological units in the study area.

3. Methods

The spatial location of the studied sedimentary columns allowed the observation of changes in the mineralogy and chemical composition of the fluvial sediments along the Guadalquivir River course. At each sampling site, a set of samples was collected from each depositional level observed within the sedimentary sequence. A description of the lithology and grain size for each sample was made both in the field and in the laboratory. The bulk samples were sieved using a 2 mm aperture size sieve in order to separate the sand, silt and clay fraction from the rest of the sample. Subsequently, the clay-sized fraction was separated using a method based on Stokes's law. Once it was obtained a dispersed suspension of clay-sized material, oriented clay aggregates were prepared.

Samples were studied using X-ray diffraction (XRD), scanning electron microscopy (SEM) with an energy dispersive X-ray (EDX) microanalyzer, and X-ray fluorescence spectrometry (XRF). XRD data were obtained from powder samples and oriented clay aggregates with a Siemens D-5000 diffractometer using CuKα radiation, Ni filter, and automatic divergence slit (University of Jaén). Clay minerals analyses were performed on three sets of oriented clay aggregates (untreated, ethylene glycol solvated, and heated at 550ºC for 2 hours). Illite/smectite mixed layers have been detected by the presence of their characteristic reflections (001/002) and (002/003) in the ethylene glycol-solvated samples, distinguishing the amount of smectite layers according to the position of their characteristic reflections (Srodon, 1984). XRD semi-quantitative analyses in the powder samples were carried out according to the standard method proposed by Snyder and Bisch (1989) and using the parameters calculated for the Siemens D-5000 diffractometer of the University of Jaén. Relative abundances of the different clay minerals were

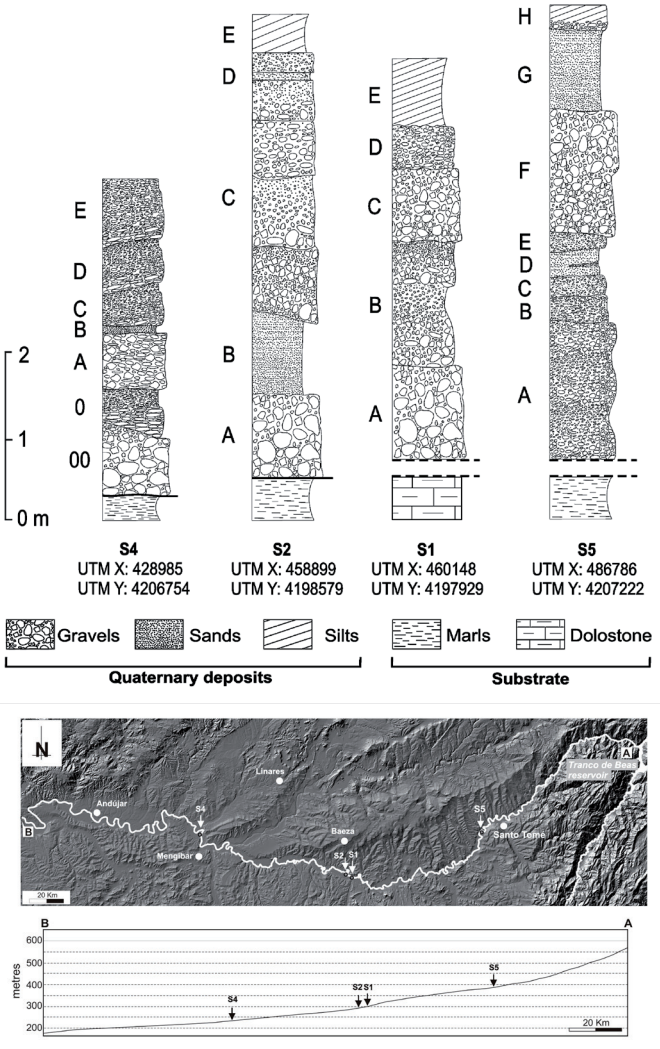

Fig. 3.- Sedimentary sequences at the four mining sites and longitudinal profile of the Guadalquivir River in the study area. The lettered sample labels are used in Tables 1 and 2.

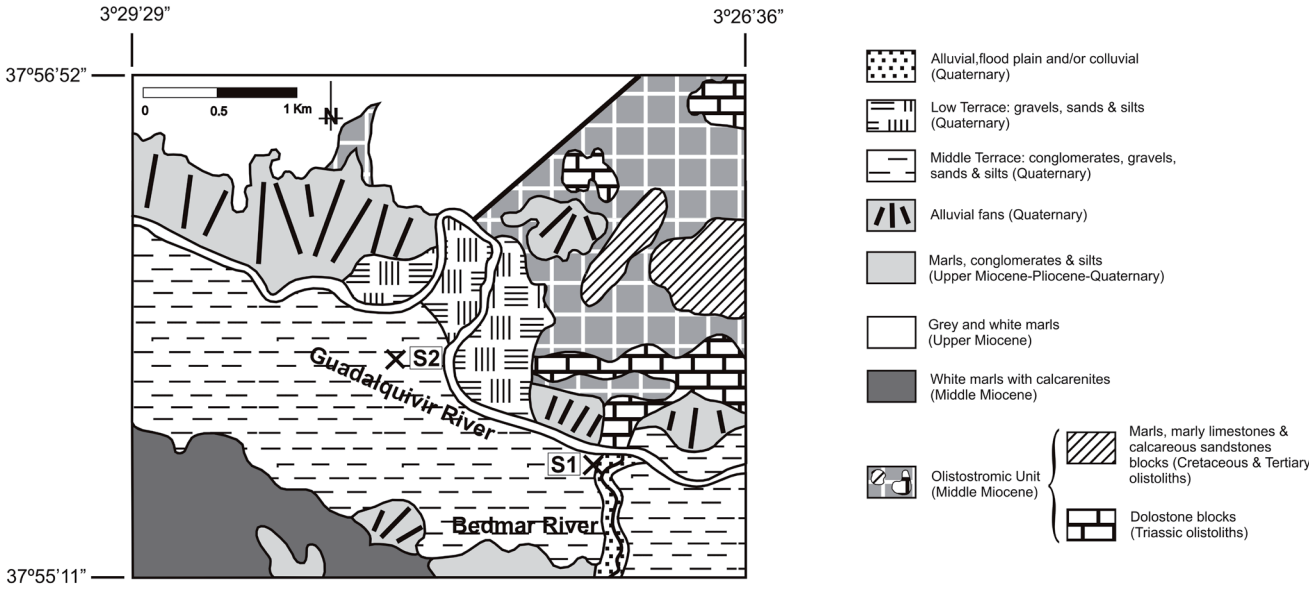

Fig. 4.- Geology map centred on the fluvial terraces of the Guadalquivir River and showing the location of the sampling sites S1 and S2.

determined using the mineral intensity factors published by Dinelli and Tateo (2001), after corrections for the automatic slit used. The quantities of smectite rich illite/smectite mixed layers were calculated using the mineral factor of smectite, while the percentages illite/smectite mixed-layer rich in illite were determined using a factor based on the intensities ratio of the reflections situated at 4.9 Å for the untreated samples and 9.4 Å for the ethylene glycol-solvated samples (Vázquez and Jiménez-Millán, 2009). The SEM study was made on polished thin sections of consolidated samples with a Jeol 5800 electron microscope equipped with a Link Isis microanalyzer at 20 kV (University of Jaén). Observations were made using backscattered electron (BSE) images in the atomic number contrast mode. For the textural and chemical characterization of phyllosilicates, sediments were prepared for transmission electron microscopy (TEM) study by two different methods. Copper rings were attached to representative selected areas of thin sections prepared with Canada balsam from consolidated samples. These areas were detached through gentle heating and further thinned with a Gatan dual ion mill. Other samples were prepared using Cu grid surface coated in a perforated formvar resin from a dispersion of finely ground sample particles, in alcohol or distilled water. The monomineralic character of each grain is proven by its electron diffraction pattern, checking the existence of a single network and, therefore, a single crystalline phase. The TEM data was obtained using the Philips CM20 (STEM) microscope, operated at 200 kV from the Scientific Instrumentation Centre (C.I.C.) of the Universidad de Granada. Quantitative analyses (AEM) of particles were obtained in STEM mode with an EDAX microanalysis system in the Philips CM20. The counting time used was 100 seconds except for Na and K, which were analysed for 15 seconds to try to minimise alkali-loss problems as short counting times improve reproducibility for K and Na (Nieto *et al.*, 1996). Chemical analyses by XRF were carried out by a Philips PW 1404/10 wavelength dispersed X-ray spectrometer equipped with a tube of rhodium of 4 kW and 30 kV. Analytical determinations were undertaken comparing with standard from synthetic oxides and natural minerals. XRF analyses were accomplished on powder from bulk samples prepared by grinding in an agate mortar. After that, pressed boric acid pellets were made using a mixture of n-butylmethacrylate and acetone as binding medium. Loss on ignition (L.O.I.) determination was carried out by comparison of the sample wet weight with the weight of the samples after heating to 1000 ºC for six hours in a furnace. Samples were cooled in a desiccator to a temperature at which they can be safely handled, then weighed. REE analyses were carried out using Inductively Coupled Plasma-Mass Spectrometry (ICP-MS) at Activation Laboratories Ltd. (Ontario, Canada).

4. Mineralogy and chemical composition of the alluvial sediments

The mineral characterization of sediments does not reveal important differences in the composition of the different grain-size fractions of individual samples. XRD analyses showed similar mineral associations in both gravel and sandy levels, that mainly consist of dolomite, calcite, quartz, clay minerals and feldspars (Table 1). The main mineralogical characteristic of these sediments is the large amount of carbonate in both, gravel and sandy levels. Calcite plus dolomite contents are higher than 40% in most of the samples. The amount of quartz varies between 5 and 65%, the lowest content were found in the samples collected at the sampling site S5. In addition, the proportion of clay minerals and feldspars is in general very low, especially in the gravel levels (frequently <5%), although significant clay mineral contents were found in some sandy levels (approximately 15% in S2

	Powder samples					Phyllosilicates in oriented aggregate samples (< 2 µm fraction)						
Sample	Cal	Dol	Qtz	Fds	Phy	Chl	Sm	Ill/Sm	Ill	Kln	Qtz	Fds
S1-B1	20	25	45	5	5	-	-	-	-	-	-	-
S1-B2	19	34	42	0	5	-	-	-	-	-	-	-
S1-B3	28	37	30	0	5	0	0	61	14	9	11	5
S1-D1	46	18	23	5	8	0	0	32	48	10	5	5
S1-E1	48	16	21	5	10	0	0	21	33	0	41	5
S2-B1	39	7	42	0	12	12	17	28	22	8	13	0
S2-B2	35	7	43	0	15	17	8	22	19	15	19	0
S2-C1	34	23	28	0	15	12	16	0	42	11	14	5
S2-C2	28	38	24	5	5	-	-	-	-	-	-	-
S2-D1	16	41	38	0	5	-	-	-	-	-	-	-
S2-D2	22	24	46	0	8	16	5	0	40	13	21	5
S2-E1	16	26	46	0	12	-	-	-	-	-	-	-
S4-0	21	24	45	5	5	0	5	0	81	5	9	0
S4-A	22	16	29	18	15	0	30	0	60	5	5	0
S4-B	26	19	30	10	15	0	41	0	44	5	10	0
S4-C	23	42	21	7	7	-	-	-	-	-	-	-
S4-D	9	16	65	5	5	0	5	0	60	16	19	0
S4-E	16	21	42	12	9	0	5	0	62	8	25	0
S5-A1	21	64	10	5	5	0	5	0	65	5	20	5
S5-A2	24	67	9	0	5	0	5	0	64	10	16	5
S5-B	22	71	7	0	5	-	-	-	-	-	-	-
S5-C	22	72	6	0	5	0	10	0	65	6	14	5
S5-D	18	69	8	5	5	0	5	0	66	15	9	5
S5-F	14	71	5	10	5	0	5	0	85	5	5	0
S5-G	29	47	19	5	5	0	5	0	79	5	11	0
S5-H	17	48	30	5	5	-	-	-	-	-	-	-

Cal: calcite; Dol: dolomite; Qtz: quartz; Fds: feldspars; Phy: phyllosilicates; Chl: chlorite; Sm: smectite; Ill/Sm: illite/smectite mixed layers; Ill: illite; Kln: kaolinite; - : no data

Table 1.- Mineralogical composition of the alluvial sediments (%). Sampling sites locations are shown in Figure 3. (S1-B: gravels; S1-D: gravels; S1-E: silts; S2-B: sands; S2-C: gravels; S2-D: sands; S2-E: silts; S4-0: gravels and sands; S4-A: gravels; S4-B: sands; S4-C: gravels; S4-D: gravels; S4-E: gravels; S5-A: gravels; S5-B: gravels; S5-C: gravels; S5-D: sands; S5-E: gravels; S5-F: gravels; S5-G: sands; S5-H: gravels and silts).

and S4 sedimentary sequences). In the alluvial sediments sampled upstream of the confluence between the Guadalquivir River and its tributary Guadiana Menor (sampling site S5) dolomite predominates over calcite. Downstream, the basal levels are rich in calcite, whereas the amount of dolomite increases upwards, being the predominant carbonate in the upper levels of the sedimentary sequences in sampling sites S2 and S4. Moreover, at the sampling site located at the confluence of the Guadalquivir River with its tributary Bedmar (sampling site S1), the basal levels of the sedimentary sequence are rich in dolomite whereas the sediments at the top are rich in calcite.

The predominant clay mineral in the Quaternary alluvial sediments of the Alto Guadalquivir basin is illite (up to 85%). Gravel levels are more illite-rich than sandy levels, in the later illite content varies between 19 and 45%. Illite shows narrow peaks in the XRD diagrams (Kübler index <0.15). Sandy levels have considerable smectite contents (8 to 21%), whereas chlorite is only present in some sandy levels from the sedimentary sequence S2 (<17%). Kaolinite can be found in almost all the samples with a maximum content of 16%. Other minerals such as quartz and feldspars are also present in the clay fraction. Clay minerals abundances also show differences between the different sampling sites, as well as discontinuous variations from bottom to top in each sedimentary sequence. The alluvial sediments at the sampling site S5 are characterized by the lowest amount of smectite plus illite-smectite mixed-layers plus chlorite. On the other hand, in S4 and S2 sites the amount of illite increases towards the top of the sedimentary sequence, whereas in S2 site the amount of smectite plus illite-smectite mixed-layers plus chlorite decreases towards the top of the sequence.

The study of consolidated samples by means of SEM (BSE images) and TEM showed similar mineral associations to those deduced from the XRD data. In the basal levels of the sedimentary sequences S2 and S4, as well as in the upper part of S1, framework is made of fragments of micrite to microsparite limestones (Fig. 5a,b) and grains of fossils. Fragments of quartz and grains of phyllosilicates can also be observed. All these grains exhibit anhedral and angular morphologies and they are included in a fine-grained matrix made of angular calcite grains and interstitial clay minerals of smectitic composition (Fig. 5c). On the other hand, anhedral and angular grains of dolomite are predominant in the framework of samples throughout the sedimentary sequence S5 and the upper levels from S2 and S4 (Fig. 5d and 5e). These grains are surrounded by a fine-grained matrix poor in phyllosilicates and containing angular dolomite and calcite grains.

AEM characterization of phyllosilicates (Table 2) revealed that dioctahedral smectites are Al-dominant (between 1.88 and 1.97 a.p.f.u. in the octahedral layer). Illite/smectite mixed-layers analyses correspond in all cases to dioctahedral compositions which octahedral sums range 0,41-0.65 a.p.f.u. Most of the trioctahedral chlorites have a high Fe/Mg ratio (>

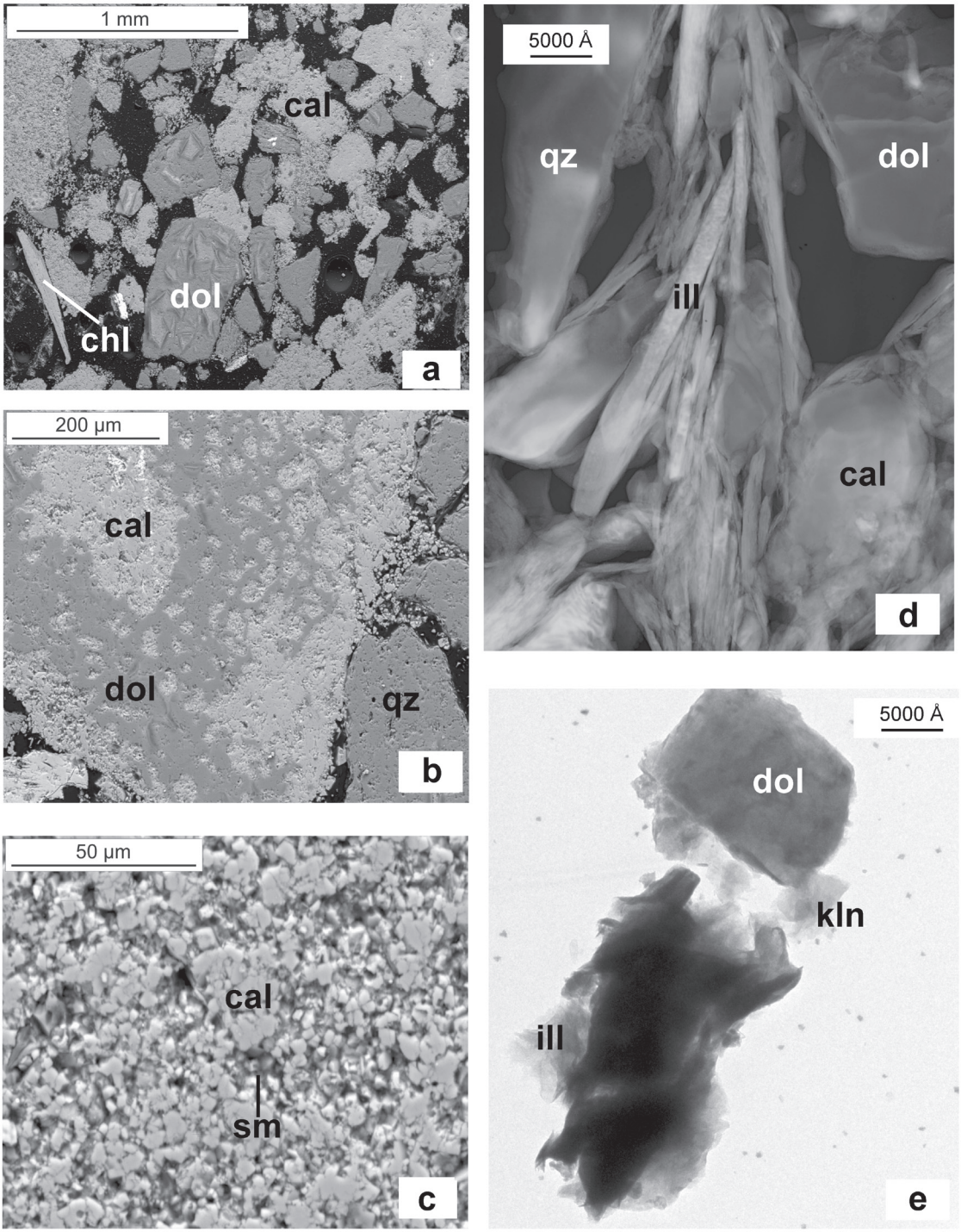

Fig. 5.- SEM-BSE (a-c) and TEM images (d-e) showing the textural and morphological features of the constituents of the framework and matrix in the studied samples.

1.44) corresponding mainly to a chamosite (Fe-rich) variety. Kaolinite showed the typical Al-rich composition. The chemical compositions of illite are characterized by a small deficit in the interlayer charge indicating that dioctahedral micas are well crystallized.

XRF data also revealed the carbonate-rich nature of the studied sediments. Loss on ignition (at 1000ºC) values vary between 16 and 40%, and CaO+MgO contents are generally >40%. Samples from S5 are MgO-enriched (>12%), whereas the highest values of CaO are found in samples from S1 and S2 (up to 44%). SiO_2 contents are generally low (>35%), although some sandy sediments from S4 contain up to 57%. The rest of the oxides of the major elements show values lower than 2.50% (Table 3).

According to the mineral and chemical composition, REE concentrations of selected samples were determined (Table 4, Fig. 6). The total REE concentration (ΣREEs) for the selected sediment samples ranged from 4.21 to 184.32 ppm.

Sample	Si	AlIV	AlVI	Fe	Mg	∑ oct.	Ca	K	Na	∑ inter.
1. S2B1-4	3.98	0.02	1.89	0.12	0.09	2.10	0.02	0.07	0.00	0.09
2. S2C1-8	3.92	0.08	1.93	0.13	0.02	2.08	0.00	0.32	0.00	0.32
3. S4B-3	3.67	0.33	1.97	0.12	0.07	2.16	0.00	0.07	0.00	0.07
4. S4C-7	3.90	0.10	1.88	0.12	0.12	2.12	0.01	0.14	0.00	0.15
5. S1B3-2	3.31	0.69	1.62	0.24	0.17	2.03		0.30	0.12	0.42
6. S1D1-6	3.35	0.65	1.46	0.28	0.41	2.15	0.06	0.51	0.05	0.62
7. S1E1-3	3.34	0.66	1.43	0.30	0.39	2,12		0.40	0.07	0.47
8. S2B1-7	3.39	0.61	1.59	0.21	0.30	2.10	0.06	0.54	0.05	0.65
9. S2B1-4	3.48	0.52	1.58	0.21	0.28	2.07		0.48	0.07	0.55
10. S2B2-9	3.52	0.48	1.68	0.16	0.23	2.07		0.38	0.03	0.41
11. S2B1-5	2.52	1.48	1.45	2.68	1.86	5.99				
12. S2B2-3	2.54	1.46	1.45	2.66	1.87	5.98				
13. S2C1-1	2.72	1.28	1.44	2.65	1.86	5.97				
14. S2D2-4	2.58	1.42	1.44	2.61	1.92	5.97				
15. S1D1-3	4.00	0.00	3.96	0.02	0.02	4.00				
16. S2B2-9	4.01	0.00	3.95	0.02	0.03	4.00				
17. S4D-1	4.00	0.00	3.98	0.01	0.01	4.00				
18. S5D-8	4.02	0.00	3.93	0.02	0.02	3.97				
19. S1D1-5	3.13	0.87	1.96	0.05	0.02	2.03	0.00	0.77	0.04	0.81
20. S2D2-4	3.14	0.86	1.93	0.06	0.04	2.03	0.01	0.69	0.16	0.85
21. S5A1-1	3.04	0.96	1.94	0.07	0.04	2.05	0.00	0.81	0.09	0.90
22. S5F-2	3.08	0.92	1.98	0.06	0.00	2.04	0.01	0.79	0.09	0.88

1-4: Smectite analyses normalized to $O_{10}(OH)_2$. 5-10: Illite/smectite mixed-layers analyses normalized to $O_{10}(OH)_2$. 11-14: Chlorite analyses normalized to $O_{10}(OH)_8$. 15-18: Kaolinite analyses normalized to $O_{10}(OH)_8$. 19-22: Illite analyses normalized to $O_{10}(OH)_2$

Table 2.- AEM representative analyses of smectite, illite/smectite mixed layers, chlorite, kaolinite and illite. (S1-B: gravels; S1-D: gravels; S1-E: silts; S2-B: sands; S2-C: gravels; S2-D: sands; S2-E: silts; S4-0: gravels and sands; S4-A: gravels; S4-B: sands; S4-C: gravels; S4-D: gravels; S4-E: gravels; S5-A: gravels; S5-B: gravels; S5-C: gravels; S5-D: sands; S5-E: gravels; S5-F: gravels; S5-G: sands; S5-H: gravels and silts).

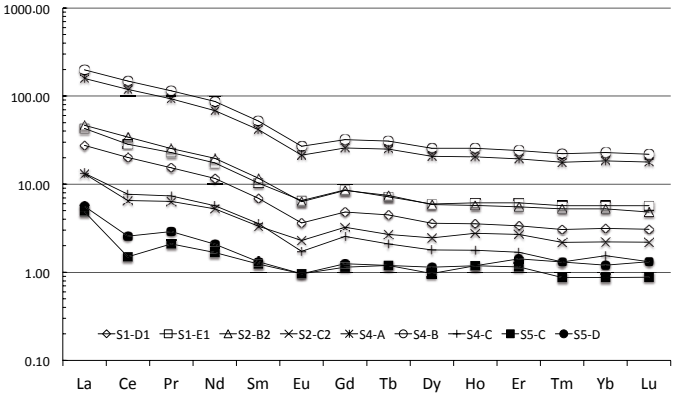

Fig. 6.- REE patterns of selected samples from the fluvial terraces.

Three groups of sediments can be distinguished according to their REE signatures:

- Sediments from sampling site S5 and upper levels from sites S2 and S4 have low ΣREE concentrations. The lowest ΣREE values are found in carbonate-rich samples from S5 site (4.21-5.96 ppm). Their flat chondrite-normalized REE patterns exhibit marked Ce and Eu depletions (Fig. 6). These depletions are less intense in sediments from upper levels of S2 and S4 sites, which have slightly higher ΣREE concentrations (14.71-12.65 ppm) than samples from S5.

- Silicate-rich from S4 site basal levels have the highest ΣREE concentrations (177.31-184.32 ppm) and exhibit chondrite-normalized REE patterns enriched in LREE and depleted in Eu. Ce depletion was not observed in these samples.

- Intermediate ΣREE concentrations are found in calcite and silicate-rich sediments from S2 site basal levels and S1 site upper levels (30.20-50.92 ppm).

5. Discussion

5.1. The detrital nature of the minerals

Calcite and dolomite are the most abundant mineral phases in the sediments. Most of the constituents of the framework and matrix that contain these minerals appear in the SEM-BSE images as isolated grains of angular morphologies. In addition, the absence of a massive formation of interstitial cements or diagenetic carbonates modifying their primary fabric and their mineralogy in both the gravel and sandy sediments of the continental deposits studied suggest that carbonates are mainly present as detrital clasts.

On the other hand, clay minerals seem also to be detrital. Even the nanometer-sized phyllosilicates display a good "crystallinity", showing well defined electron diffraction, and suggesting that they were formed by physical degradation mechanisms such as grain-size reduction. Additionally, illite peaks in the XRD diagrams are narrow, which suggests that phyllosilicates are likely to be a product of physical weathering of the rocks in the source areas. Illite has been found to be a detrital product of erosional processes of many continental rocks that contained micas (Biscaye, 1965; Moriarty, 1977; Chamley, 1989; Ehrmann *et al.*, 1992). The presence of very small amount of kaolinite also indicate that chemical

Sample	SiO_2	Al_2O_3	Fe_2O_3	MgO	CaO	Na_2O	K_2O	TiO_2	LOI
S1-B1	31.14	1.17	1.24	9.23	33.51	0.54	0.45	0.21	22.64
S1-B2	30.92	0.59	1.22	10.21	29.56	0.43	0.53	0.17	26.21
S1-B3	21.45	0.71	0.65	11.01	37.21	0.31	0.21	0.08	28.32
S1-D1	18.01	1.11	2.01	6.71	44.21	0.23	0.31	0.10	27.39
S1-E1	17.19	1.14	1.98	5.98	45.30	0.09	0.17	0.13	28.01
S2-B1	30.65	1.22	1.24	6.17	42.92	0.72	0.31	0.21	20.11
S2-B2	31.01	1.31	1.34	6.21	39.01	0.69	0.41	0.15	19.82
S2-C1	21.42	1.16	1.54	9.02	41.23	0.71	0.67	0.09	23.32
S2-C2	21.73	1.19	0.67	10.23	32.45	0.47	0.63	0.11	32.31
S2-D1	31.09	1.21	0.52	11.51	29.41	0.54	0.41	0.12	25.21
S2-D2	32.00	1.31	0.24	8.24	28.45	0.61	0.72	0.56	27.45
S2-E1	31.76	1.28	0.29	9.51	28.18	0.78	1.01	0.35	26.33
S4-0	32.37	1.05	1.08	9.51	32.05	0.68	0.54	0.43	22.17
S4-A	25.45	2.34	1.74	9.03	34.54	1.21	1.01	0.54	24.09
S4-B	26.01	2.11	1.81	9.51	35.02	0.78	0.69	0.23	23.47
S4-C	20.98	0.65	0.67	12.03	32.52	0.51	0.72	0.19	31.62
S4-D	57.21	1.23	0.44	6.76	15.98	0.65	0.81	0.92	16.24
S4-E	49.06	2.32	0.41	7.51	15.76	0.76	1.02	0.74	22.14
S5-A1	12.23	1.17	0.21	14.44	32.34	0.21	0.77	0.21	38.24
S5-A2	11.95	1.14	0.18	15.01	31.65	0.17	0.67	0.18	39.04
S5-B	10.62	1.21	0.18	17.11	30.58	0.21	0.71	0.24	39.21
S5-C	10.42	1.01	0.15	17.03	30.64	0.29	0.83	0.16	39.56
S5-D	11.48	1.31	0.21	16.78	30.37	0.11	1.21	0.15	38.48
S5-F	10.01	1.39	0.18	17.31	30.58	0.21	0.91	0.13	37.72
S5-G	21.72	0.67	0.71	12.03	32.12	0.41	0.92	0.19	31.27
S5-H	21.53	1.19	0.77	12.54	32.85	0.52	1.02	0.21	29.25

LOI: Loss on ignition, 1000 ºC

Table 3.- Chemical composition of the alluvial sediments (wt. %). Sampling sites locations are shown in Figure 3. (S1-B: gravels; S1-D: gravels; S1-E: silts; S2-B: sands; S2-C: gravels; S2-D: sands; S2-E: silts; S4-0: gravels and sands; S4-A: gravels; S4-B: sands; S4-C: gravels; S4-D: gravels; S4-E: gravels; S5-A: gravels; S5-B: gravels; S5-C: gravels; S5-D: sands; S5-E: gravels; S5-F: gravels; S5-G: sands; S5-H: gravels and silts).

Sample	La	Ce	Pr	Nd	Sm	Eu	Gd	Tb	Dy	Ho	Er	Tm	Yb	Lu	ΣREEs
S1-D1	6.52	12.30	1.43	5.31	1.03	0.21	0.96	0.16	0.89	0.19	0.54	0.08	0.51	0.08	30.20
S1-E1	10.16	17.43	2.12	7.97	1.52	0.37	1.72	0.26	1.47	0.33	0.98	0.14	0.92	0.14	45.52
S2-B2	11.02	21.06	2.35	9.01	1.73	0.36	1.68	0.27	1.45	0.31	0.89	0.13	0.84	0.12	50.92
S2-C2	3.10	4.01	0.59	2.40	0.50	0.13	0.65	0.10	0.60	0.15	0.43	0.05	0.36	0.05	12.65
S4-A	37.58	72.90	8.61	31.32	6.15	1.20	5.12	0.90	5.11	1.11	3.09	0.44	2.97	0.44	177.31
S4-B	47.13	90.69	10.67	39.72	7.70	1.52	6.37	1.11	6.28	1.39	3.84	0.55	3.68	0.54	184.32
S4-C	3.16	4.70	0.68	2.60	0.53	0.10	0.51	0.08	0.44	0.10	0.27	0.03	0.25	0.03	14.71
S5-C	1.16	0.92	0.19	0.77	0.18	0.05	0.23	0.04	0.24	0.06	0.18	0.02	0.14	0.02	4.21
S5-D	1.33	1.58	0.27	0.95	0.19	0.05	0.25	0.04	0.28	0.06	0.23	0.03	0.19	0.03	5.96

Table 4.- REE concentrations of selected samples from the alluvial sediments (p.p.m.). Sampling sites locations and sampling deposit labels are shown in Figure 3.

weathering was very limited. Moreover, the dioctahedral Al–Fe composition of the clay minerals observed in the studied sediments is within the characteristic compositional range of the clay minerals present in rocks from the surrounding areas such as the marly Miocene sediments of the Guadalquivir basin (González *et al.*, 1998) and the marls and limestones from the Subbetic domain of the External Zones of the Betic Cordillera (Palomo, 1987; Ortega-Huertas *et al.*, 1991).

Therefore, XRD and electron microscope data indicate that the mineral assemblages of the alluvial sediments of the Alto Guadalquivir Basin mainly consist of detrital phases. Textural grain microfeatures (angular edges, absence of cements) and good crystallinities can be correlated with physical degradation, such as grain size diminution, short transport and fast physical deposition processes. This is extremely useful in order to explain the mineralogical and geochemical variations deduced from XRD, SEM, TEM, XRF and ICP-MS data and their relation to the provenance of the alluvial sediments.

5.2. Mineralogical assemblages, geochemical signatures and source areas

Mineral assemblages of sedimentary rocks are strongly controlled by source rock compositions, physical-chemical weathering, transport and depositional mechanisms (Damiani *et al.*, 2006), which may determine a selective enrichment of the different mineralogical phases. Mineralogy and major element data can provide information to distinguish among different type of sediments in a basin. Dinis and Oliveira (2016) indicated that the relations between SiO_2, Al_2O_3, quartz and kaolinite contents reflect the differentiation between quartz-rich and phyllosilicate-rich sediments from the West Iberia

Atlantic Margin. Determination of immobile elements is the key to mass transport calculations during weathering and hydrothermal alteration (Gong *et al.*, 2011). For mature sediments formed from materials that underwent advanced processes of chemical weathering and recycling, the determination of mobile and immobile elements is appropriated to deduce relevant provenance indicators (e.g. Dinis and Oliveira, 2016). For inmature sediments where the physical weathering and deposition were the prominent processes, immobile element is just a relative notion (Gong *et al.*, 2011), and traditionally considered immobile elements such as Ti and Al can be often subjected to significant fractionation during sediment transport and deposition (Goudie, 2004). However, these effects can be almost neglected under short-transport and fast-deposition conditions, such as those from upperstream part of uplifting alluvial basins (Riebe *et al.*, 2004). In the study area, given that XRD and electron microscope characterization point to physical degradation, short transport and fast physical deposition processes as prominent, sediment mineral assemblages and major element composition can be attributed to variations in the geological features of the drainage area and/or to changes in the relative influence of source areas. Two main types of mineralogical assemblages in the alluvial sediments of the Alto Guadalquivir: (i) assemblages rich in calcite, smectite and illite/smectite mixed-layers, and (ii) dolomite and illite-rich assemblages.

In order to integrate the sedimentological, mineralogical and geochemical data obtained during this work we carried out a principal components analysis (PCA). To undertake the PCA, the SPSS factor analysis module (SPSS Inc., 2005) was used, specifying the principal components method with *varimax* rotation (Kaiser, 1958). The rotation of the components axis is performed so that components are clearly defined by high loadings for some variables and low loadings for others, facilitating the interpretation in terms of original variables. R-mode principal components analysis (Jiménez-Espinosa, 2003) was undertaken on the following variables: calcite, dolomite, quartz, feldspars, phyllosilicates, illite, SiO_2, TiO_2, Al_2O_3, Fe_2O_3, MgO, CaO, K_2O, Na_2O, IS, and LOI (loss on ignition). Smectite, illite/smectite mixed-layers and chlorite contents were combined to obtain the variable IS. REE data were not included in the statistical treatment because we had only analyses of selected samples. Extracting two components during the analysis was sufficient to account for approximately 70% of the variation in the dataset, then a component loading table (Table 5) was produced to show the strength of the relationship between each variable and component. Subsequently, the two components were used to generate two corresponding groups of *component scores* by multiplying the original observations by the appropriate component-score coefficients (Table 6).

The first principal component (PC1) accounts for about 46% of the variance in the original data and shows the association of two groups of variables (Table 5). The first group of variables includes calcite, the sum of smectite+illite/smectite+chlorite, Fe_2O_3, CaO and the whole content of phyllosilicate minerals. Samples from the basal part of the sedimentary sequence S2 and the upper part of S1 showed the highest positive scores on this component (Table 6). This group of variables can be related to source areas containing high amounts of marls rich in phyllosilicate minerals with a smectitic component and/or limestones, such as the local marly Neogene lithological units of the Guadalquivir Basin and the Mesozoic Subbetic limestone-rich lithological unit of Sierra Mágina located to the south of the study area. On the other hand, dolomite, illite, K_2O, MgO and LOI have high

Table 5.- Loading values for varimax rotated principal components (PCs) applied to the studied geochemical and mineralogical variables.

Variable	PC1	PC2
Cal	0.89	-0.21
IS	0.84	0.11
Fe_2O_3	0.79	0.25
CaO	0.81	-0.47
Phy	0.69	0.58
K_2O	-0.86	0.14
Ill	-0.84	-0.10
Dol	-0.69	-0.71
MgO	-0.69	-0.66
LOI	-0.51	-0.82
SiO_2	0.05	0.91
TiO_2	-0.36	0.86
Qtz	0.29	0.84
Na_2O	0.16	0.83
Al_2O_3	-0.13	0.66
Fds	-0.27	0.50

Cal: calcite; IS: Smectite + illite/smectite mixed layers + chlorite; Phy: phyllosilicates; Ill: illite; Dol: dolomite; LOI: loss on ignition; Qtz: quartz; Fds: feldspars.

Table 6.- Principal component scores. (S1-B: gravels; S1-D: gravels; S1-E: silts; S2-B: sands; S2-C: gravels; S2-D: sands; S2-E: silts; S4-0: gravels and sands; S4-A: gravels; S4-B: sands; S4-C: gravels; S4-D: gravels; S4-E: gravels; S5-A: gravels; S5-B: gravels; S5-C: gravels; S5-D: sands; S5-E: gravels; S5-F: gravels; S5-G: sands; S5-H: gravels and silts.

Sample	PC1 scores	PC2 scores
S1-B1	–	–
S1-B2	–	–
S1-B3	1.04	-0.69
S1-D1	1.31	-0.52
S1-E1	1.48	-0.61
S2-B1	1.55	0.25
S2-B2	1.40	0.38
S2-C1	0.95	-0.05
S2-C2	–	–
S2-D1	–	–
S2-D2	-0.09	0.64
S2-E1	–	–
S4-0	-0.20	0.60
S4-A	-0.11	1.47
S4-B	0.54	0.74
S4-C	–	–
S4-D	-0.90	1.95
S4-E	-1.08	1.93
S5-A1	-0.72	-0.83
S5-A2	-0.59	-1.05
S5-B	–	–
S5-C	-0.74	-1.10
S5-D	-1.09	-0.85
S5-F	-1.20	-0.77
S5-G	-0.48	-0.46
S5-H	–	–

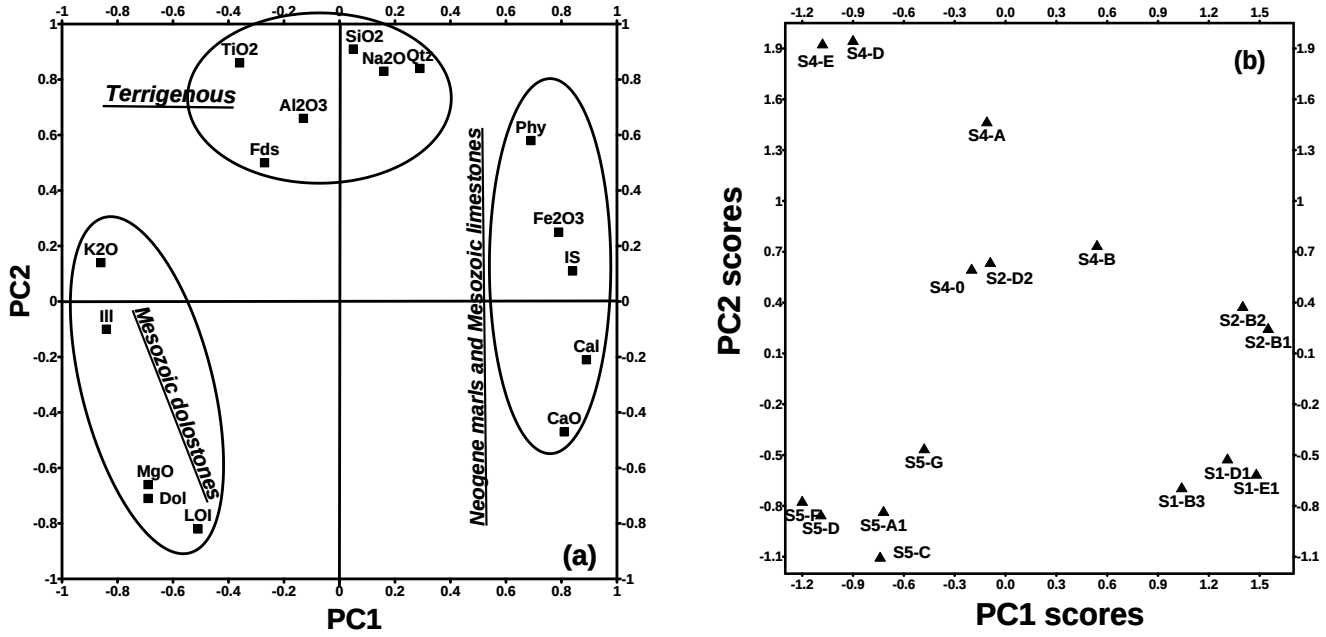

Fig. 7.- (a) Plot of the loading values for principal components of the PCA representing different associations of variables; (b) plot of the sample scores in the principal component 1 and 2.

negative loadings on this component. These variables can be related to a source area enriched in dolostones in which the main phyllosilicate is illite, such as the material forming the Mesozoic Prebetic Sierra de Cazorla and the dolomitic Triassic blocks included in the Neogene Olistrostomic unit of the Guadalquivir Basin. Samples throughout the sedimentary sequence S5 and the upper part of S2 and S4 have negative scores on this component (Table 6). The second component (PC2) explains about 30% of the variance in the original data. The variables SiO_2, TiO_2, quartz, Na_2O, Al_2O_3 phyllosilicates and feldspars have high positive loadings on this component, whereas the variables LOI, dolomite, and MgO have high negative loadings on it (Table 5). The terrigenous nature of the association quartz, feldspars, SiO_2, TiO_2, Na_BO and Al_2O_3, the negative correlation of this group of variables with those representing the deposition of carbonates and the significant positive scores of some samples from the upper part of the sedimentary sequence S4 on PC2, suggest that this component represents the influence of the sedimentary processes that led to the deposition of the Paleozoic silicate-rich sediments from the Sierra Morena area transported by the Guadalimar River (Fig. 2).

Our results indicate that typically considered immobile elements such as Ti and Al are statistically associated to the presence of terrigenous mineral assemblages, whereas that Ca and Mg, typically considered highly mobile major elements, defines two contrasting statistical groups: one for calcite rich assemblages and the other for dolomite rich assemblages (Fig. 7), revealing that distribution of elements can be more correctly interpreted according to source areas than fractionation processes produced by chemical weathering, transport or deposition. Rare earth elements (REEs) have been used to trace the provenance of various sediments and interpret sedimentary changes (Henderson, 1984, Magee *et al.*, 1995; Stevens and Quinton, 2008). Limestone and other carbonate rocks are characterized by low REE concentrations, flat chondrite-normalized patterns and Ce depletion (Balashov and Girin, 1969). In the studied sediments, these features are controlled by their carbonate content, indicating an intense carbonate effect on the REE geochemistry associated to the material provenance. The REEs concentration and fractionation varies in the sediments according to the proportion among carbonates and silicates. REE signature of sediments from sampling site S5 and upper levels from sites S2 and S4 is in agreement with the composition of the dolostones from the Sierra de Cazorla tectonic flakes, representing proximal source area deposits placed at the headwaters of the Guadalquivir river. In the rest of sediments, elevated ΣREEs values can be related to the relative reduction of carbonates in the sediments and the increase of silicate material produced and concentrated during soil formation processes in the neighbouring source areas. Lei *et al.* (1994) reported increasing LREE/HREE with REE enrichment in sediments produced by weathering of carbonate rock in drainage. Clay minerals formed during the weathering processes absorb greater LREE than HREE in alkaline environments (Wen *et al.*, 2014). The transport of these products into the alluvial sediments led to an increase of their REE contents and LREE/HREE ratios. This process produced the moderate REE contents and slight LREE enrichment observed in the alluvial sediments associated to the source area made of Neogene marls Mesozoic limestones near Sierra Mágina. However, the highest ΣREE concentrations and chondrite-normalized REE patterns enriched in LREE found in sediments from S4

site basal levels can be associated to materials coming from soil formation in the Sierra Morena Paleozoic source area (made of metamorphic and plutonic rocks) transported to the alluvial deposits by the Guadalimar River. Therefore, the flat chondrite-normalized REE patterns or slightly enriched in LREE reveal the absence of important fractionation processes during the weathering, transport and deposit of the studied deposit, which is in agreement with its commonly accepted immobile behaviour and points to the source rock as main factor controlling the composition of the alluvial sediments in the study area.

The obtained results showed the existence of significant differences in the chemical composition of the sediments and in the distribution of the carbonate, quartz, feldspars and clay mineral assemblages between the four sedimentary sequences, which allowed identifying the existence of two main provenance signatures during the evolution in the deposition of the Quaternary alluvial sediments of the Alto Guadalquivir. These results suggest that (i) most of the alluvial sediments enriched in calcite and smectite come from the Neogene sediments that comprise the substrate of the Guadalquivir basin and the Mesozoic Subbetic rocks of Sierra Mágina, and that (ii) the main source of the dolomitic and illitic fraction of the alluvial sediments come from the Mesozoic Prebetic rocks of Sierra de Cazorla and the blocks containing Triassic sediments included in the Olistrostromic unit of the Guadalquivir Basin. The influence of Sierra Morena as a source area was only observed in the sedimentary sequence S4. This sequence is located downstream of the confluence between the Guadalquivir River and its tributary Guadalimar which drains the lithological units comprising Sierra Morena.

5.3. Variations in the provenance of the alluvial sediments: geomorphological processes and erosion/deposition rates.

Alluvial sediments composition is controlled by the relief, drainage systems, climate and tectonic environment of the source area as well as along the river course (Mehl *et al.*, 2012; Palamakumbura and Robertson 2016). The geomorphological characteristics of the study area and, especially, the important difference in height between the middle and higher terraces of the alluvial sediments (see section 2) suggests a first stage in the evolution of the fluvial system in which the valley incision and the erosion of the Neogene materials of the Guadalquivir Basin were the predominant processes. Grain microfeatures, sub-angular in outline with medium to low relief and abrupt edges can be considered as representative of alluvial grains that were exposed to short low-energy subaqueous transport favouring proximal deposits near and within the source area. Moreover, the poor development of the upper terrace in the study area indicates that those processes continued after its formation. Consequently, during the first stages of aggradation of the middle terrace most of the sediments would consist of Neogene materials. This is consistent with the calcitic and smectitic composition of the sediments corresponding to the basal levels of the sedimentary sequences S2 and S4, which overlie the late Tortonian and Messinian units, respectively, as well as the dolomitic and illitic composition of the sediments at the base of the sedimentary sequence S1, which overlies a block of Triassic dolostones of the Olistostromic unit. Therefore, the lithology of the bedrock directly incised by the river seems to be the main factor controlling the composition of the basal sediments of the middle terrace.

Thus during the aggradation of the middle terrace deposition predominates over erosion and incision processes. Once the middle terrace was sufficiently aggradated a change in the fluvial system dinamics took place that promoted the deposition of sediments transported from the surrounding source areas. The mineralogical and chemical composition of the sediments at the upper parts of the sedimentary sequences suggests that the sediments were mainly delivered from the carbonate-rich Betic front. The predominance of this source area over northern margin of the basin (Sierra Morena) is due to its higher altitude, with high slope gradients for the tributaries that drain the western margin of the Guadalquivir River. The asymmetry between the northern margin (Sierra Morena) and the southern margin (Betic front) is the result of the important uplift of the Betic front caused by the neotectonic activity (Sanz de Galdeano and Alfaro, 2004), which is thought to be still ongoing in certain sectors of the front. This uplift was responsible of the change in the fluvial system dinamics that took place once the middle terrace was sufficiently aggradated. The upper levels of the sedimentary sequences S2 and S4 in the south-western as well as the sediments throughout the sedimentary sequence S5 in the north-eastern sector of the study area received dolomite-rich sediments transported from the Sierra de Cazorla. Therefore, weathering and erosion of the Sierra de Cazorla dolostone sequences produced a significant increase of the amount of dolomitic materials transported by the river in this segment. On the other hand, the increase in calcite-rich sediments towards the top of the sedimentary sequence S1 (located at the confluence between the Guadalquivir River and its tributary Bedmar) can be interpreted as the result of the sediment influx supplied by the Bedmar River draining the limestone-rich mountains comprising Sierra Mágina. The small influence of the Paleozoic silicate-rich materials delivered from the northern margin (Sierra Morena) can only be observed in the upper levels of the sedimentary sequence S4, located downstream of the confluence between the Guadalquivir River and its tributary Guadalimar which drains the lithological units comprising Sierra Morena.

6. Conclusions

The results of this study have provided important information about how mineral and geochemical characterization in-

tegrated with sedimentary and geomorphological data allow the identification of the factors that control changes in the source areas of the alluvial sediments that composed the sedimentary sequence of the Alto Guadalquivir Basin:

1. Mineral characterization and geomorphological setting of the alluvial sediments of the Alto Guadalquivir Basin point to physical degradation, short transport and fast physical deposition as prominent processes involved in its origin. Statistical association among mineral assemblages and chemical composition of these sediments reveal that element fractionation effects can be almost neglected and element distribution can be interpreted according to the influence of the source areas.

2. Most of the materials rich in CaO, calcite, smectite and illite/smectite mixed-layers come from the marly substrate of the Guadalquivir basin and limestones from Mesozoic Subbetic sequences of Sierra Mágina

3. MgO, dolomite and illite-rich materials of the alluvial sediments come from the Mesozoic Prebetic rocks of Sierra de Cazorla and the blocks containing Triassic sediments included in the Olistrostromic unit of the Guadalquivir Basin.

4. The important incision represented the very upper fluvial terrace indicates an initial predominantly erosive stage of the fluvial system where Neogene bedrock materials of calcitic and smectitic composition were deposited at the base of the middle terrace.

5. After the main stage of aggradation of the middle terrace was sufficiently achieved the deposition of sediments delivered from the carbonate-rich Betic front of the surrounding source areas predominated over the erosion and incision of the substrate.

Acknowledgements

We acknowledge the suggestions and comments of the editors and two anonymous reviewers. Funding assistance was provided by the Junta de Andalucía (Research Group RNM-325), University of Jaén, and project "Complex rheologic behaviour of active fault zones in carbonate multilayer sequences: applications to the estimation of seismic hazard and the exploitation of water" (University of Jaen).

References

Anderson, J.B., Ashley G.M. (1991): Glacial marine sedimentation: paleoclimatic significance; a discussion. *Geological Society of America Bulletin Special Paper* 261, 223–226.

Armijo, R., Benkhelil J., Bousquete, J.C., Estévez, A., Guiraud, R., Montenat C.H., Pavillon, M.J., Philip, H., Sanz De Galdeano, C. Viguier C.I. (1977): Les résultats de l'analyse structurale en Espagne. In: L'histoire tectonique récent (Tortonien à Quaternaire) de l'Arc de Gibraltar et des bordures de la mer d'Alboran. *Bulletin de la Societé Géologique de France* 19, 591–594.

Baena, R. (1993): *Evolución cuaternaria (3 M.a) de la Depresión del Medio-Bajo Guadalquivir y sus márgenes (Córdoba y Sevilla)*. Tesis Doctoral, Univ. de Sevilla. 589 p.

Balashov, Y.A., Girin, Y.P. (1969): On reserve of mobile rare earth elements in sedimentary rocks. *Geochemistry International* 6, 649-658.

Bayhan, E. (2005): Tertiary clay mineralogy of the Cokelezdag region (NE Denizli-SW Turkey): origin and provenance. *Journal of the Geological Society of India* 66, 21–27.

Benkhelil, J. (1976): *Etude néotectonique de la terminaision occidentale des Cordillères Bétiques (Espagne)*. Thèse 3ème Cycle, University of Nice.

Biscaye, P.E. (1965): Mineralogy and sedimentation of recent deep-sea clay in the Atlantic Ocean and adjacent seas and oceans. *Geological Society of America Bulletin* 76, 803–832.

Blank, R.G., Margolis, S.V. (1975): Pliocene climatic and glacial history of Antarctica as revealed by Southeast Indian Ocean deep-sea cores. *Geological Society of America Bulletin* 86, 1058–1066.

Caracciolo, L., Garzanti E., Von Eynatten H., Weltje G.J. (2016): Sediment generation and provenance: processes and pathways. *Sedimentary Geology* 336, 1-2. doi:10.1016/j.sedgeo.2016.03.015

Chamley H. (1989): *Clay Sedimentology*. Springer Verlag, Berlin.

Damiani, D., Giorgetti, G., Memmi, I. (2006): Clay mineral fluctuations and surface textural analysis of quartz grains in Pliocene–Quaternary marine sediments from Wilkes Land continental rise (East-Antarctica): Paleoenvironmental significance. *Marine Geology* 226, 281-295. doi:10.1016/j.margeo.2005.11.002

Dinelli, E., Tateo, T. (2001) Sheet silicates as effective carriers of heavy metals in the ophiolitic mine area of Vigonzano (northern Italy). *Mineralogical Magazine* 65, 121-132.

Dinis, P., Oliveira, A. (2016): Provenance of Pliocene clay deposits from the Iberian Atlantic Margin and compositional changes during recycling. *Sedimentary Geology* 336: 171-182. doi:10.1016/j.sedgeo.2015.12.011.

Ehrmann, W.U., Grobe, H., Fütterer D.K. (1992): Late Miocene to Holocene glacial history of East Antarctica revealed by sediments from Sites 745 and 746. *Proceedings of the Ocean Drilling Program, Scientific Results* 119, 239–260.

Gingele, F.X., De Deckker, P. (2004): Fingerprinting Australia's rivers with clay minerals and the application for the marine record of climate change. *Australian Journal of Earth Sciences* 51, 339–348. doi: 10.1111/j.1400-0952.2004.01061.x.

García Tortosa, F.J., Sanz De Galdeano, C., Alfaro, P., Jiménez Espinosa, R., Jiménez Millán, J., Lorite Herrera, M. (2008): New evidence about the age of the endorheic-exorheic transition of the Guadix-Baza basin. *Geogaceta* 44, 211-214.

Gong, Q., Deng, J., Yang, L., Zhang, J., Wang, Q., Zhang, G. (2011): Behavior of major and trace elements during weathering of sericite–quartz schist. *Journal of Asian Earth Sciences* 42, 1-13. doi:10.1016/j.jseaes.2011.03.003.

Goudie, A.S. (2004): *Encyclopedia of Geomorphology*. Routledge NY, USA.

González, I., Galán, E., Miras, A., Aparicio, P. (1998): New uses for brick-making clay materials from the Bailén area (southern Spain). *Clay Minerals* 33, 453−465.

Grobe, H., Mackensen, A. (1992): Late Quaternary climatic cycles as recorded in sediments from the Antarctic continental margin. *Antarctic Research Series* 56, 349–376.

Henderson, P. (1984): *General geochemical properties and abundances of the rare earth elements.* Elsevier, New York.

Jiménez-Espinosa, R. (2003): Tratamiento numérico de la información hidrogeológica: fases de estudio y ejemplos de aplicación. *Boletín Geológico y Minero* 114, 311−322.

Jiménez-Espinosa, R., Jiménez-Millán, J. (2003): Calcrete development in mediterranean colluvial carbonate systems from SE Spain. *Journal of Arid Environments* 53, 479–489. Doi:10.1006/jare.2002.1061.

Kaiser, H.F. (1958): The varimax criteria for analytical rotation in factor analysis. *Psychrometrika* 23, 187–200.

Magee, J.W., Bowler, J.M., Miller, G.H., Williams, D.L.G. (1995): Stratigraphy, sedimentology, chronology and palaeohydrology of Quaternary lacustrine deposits at Madigan Gulf, Lake Eyre, south Australia. *Palaeogeogr Palaeoclimatol* 113, 3-42.

Mehl, A., Blasi, A., Zárate, M. (2012): Composition and provenance of Late Pleistocene–Holocene alluvial sediments of the eastern Andean piedmont between 33 and 34° S (Mendoza Province, Argentina). *Sedimentary Geology* 280, 234-243. doi:10.1016/j.sedgeo.2012.05.011.

Moore, M.D., Reynolds R.C. (1989): *X-ray diffraction and the identification and analysis of clay minerals.* Oxford University Press, New York.

Moriarty, K.C. (1977): Clay minerals in southeast Indian Ocean sediments, transport mechanisms and depositional environments. *Marine Geology* 25, 149–174.

Müller, C., Stein R. (2000): Variability of fluvial sediment supply to the Laptev Sea continental margin during Late Weichselian to Holocene times: implications from clay-mineral records. *International Journal of Earth Sciences 89*, 592–604. doi:10.1007/s005310000112.

Ortega-Huertas, M., Palomo, I., Moresi, M., Oddone M. (1991): A mineralogical and geochemical approach to establishing a sedimentary model in a passive continental margin (Subbetic Zone, Betic Cordilleras, SE Spain). *Clay Minerals* 26, 389–407.

Palamakumbura, R.N., Robertson A.H.F. (2016): Pleistocene terrace deposition related to tectonically controlled surface uplift: An example of the Kyrenia Range lineament in the northern part of Cyprus. *Sedimentary Geology* 339, 46-67. doi:10.1016/j.sedgeo.2016.03.022.

Prizomwala, S.P., Bhatt, N. And Basavaiah, N. (2014): Provenance discrimination and Source-to-Sink studies from a dryland fluvial regime: An example from Kachchh, western India. *International Journal of Sediment Research* 29, 99-109. doi:10.1016/S1001-6279(14)60025-1.

Palomo, I. (1987): *Mineralogía y geoquímica de sedimentos pelágicos del Jurásico inferior de las Cordilleras Béticas (SE de España).* Tesis doctoral. Universidad de Granada.

Riebe, C.S., Kirchner J.W., Finkel, R.C. (2004): Sharp decrease in long-term chemical weathering rates along an altitudinal transect. *Earth and Planetary Science Letters* 218, 421-434. doi:10.1016/S0012-821X(03)00673-3.

Roldán, F.J. (1995): Evolución neógena de la Cuenca del Guadalquivir. Tesis Doctoral. Universidad de Granada.

Santos-García, J.A., Jerez-Mir, F., Saint-Aubin, J. (1991): Estudio sedimentológico de un sector del río Guadalquivir en las proximidades de Andújar (Provincia de Jaén). Los depósitos de la terraza +6m (T4). *Estudios Geológicos* 47, 43−55.

Sanz De Galdeano, C. (1990): Geologic evolution of the Betic Cordilleras in the Western Mediterranean, Miocene to the present. *Tectonophysics* 173 , 175–178.

Sanz De Galdeano, C., Alfaro, P. (2004): Tectonic significance of the present relief of the Betic Cordillera. *Geomorphology* 63, 175–190. doi:10.1016/j.geomorph.2004.04.002.

Sanz De Galdeano, C., López-Casado, C. (1988): Fuentes sísmicas en el ámbito bético-rifeño. *Revista de Geofísica* 44, 175–198.

Snyder, R.L., Bisch, D.L. (1989): Quantitative analysis. Modern Powder Diffraction. *Reviews in Mineralogy* 20, 100−275.

Srodon, J. (1984): Mixed layer illite-smectite in low temperature diagenesis: data from the Miocene of the Carpathian foredeep. *Clay Minerals* 19, 2015-215.

Stevens, C.J., Quinton, J.N. (2008): Investigating source areas of eroded sediments transported in concentrated overland flow using rare earth element tracers. *Catena* 74, 31-36. doi:10.1016/j.catena.2008.01.002.

Stokes, M., Mather, A.E. (2000): Response of Plio-Pleistocene alluvial systems to tectonically induced base-level changes, Vera Basin, SE Spain. *Journal of the Geological Society of London* 157, 303–316. doi: 10.1144/jgs.157.2.303.

Tucker, G.E., Slingerland, R., (1996): Predicting sediment flux from fold and thrust belts. *Basin Research* 8, 329–349.

Vázquez, M and Jiménez Millán, J (2009): Suitability of the Betic Cordillera marly materials for the manufacture of pressed tile. *Materiales de Construcción* 59, 294, 97-112. doi: 10.3989/mc.2009.47707.

Viguier, C. (1977): Les grands traits de la tectonique du Basin Neogene du Bas Guadalquivir. *Boletín Geológico y Minero* 88, 39–44.

Wen, X.Y., Huang, C.M., Tang, Y., Gong-Bo, S.L., Hu, X.X. And Wang, Z.W. (2014): Rare earth elements: a potential proxy for identifying the lacustrine sediment source and soil erosion intensity in karst areas. *J. Soils Sediments* 14, 1693-1702. doi: 10.1007/s11368-014-0928-y.

Whitmore, G.P., Crook, K.A.W., Johnson, D.P. (2004): Grain size control of mineralogy and geochemistry in modern river sediment, New Guinea collision, Papua New Guinea. *Sedimentary Geology* 171, 129–157. doi:10.1016/j.sedgeo.2004.03.011

Yoon, H.I., Park, B.K., Kim, Y., Kim, D. (2000): Glaciomarine sedimentation and its paleoceanographic implications along the fjord margin in the South Shetland Islands, Antarctica during the last 6000 years. *Palaeogeography, Palaeoclimatology, Palaeoecology* 157, 189–211. doi:10.1016/S0031-0182(99)00165-0.